Syntheses and Micellar Properties of Well-Defined Amphiphilic AB_2 and A_2B Y-Shaped Miktoarm Star Copolymers of ε-Caprolactone and 2-(Dimethylamino)ethyl Methacrylate

HAO LIU,[1] JIAN XU,[1] JIALI JIANG,[1] JUN YIN,[1] RAVIN NARAIN,[2] YUANLI CAI,[3] SHIYONG LIU[1]

[1]Department of Polymer Science and Engineering, Hefei National Laboratory for Physical Sciences at the Microscale, University of Science and Technology of China, Hefei, Anhui 230026, China

[2]Department of Chemistry and Biochemistry, Laurentian University, Sudbury, Ontario, Canada P3E 2C6

[3]College of Chemistry, Xiangtan University, Xiangtan, Hunan 411105, China

Received 22 September 2006; accepted 23 November 2006
DOI: 10.1002/pola.21915
Published online in Wiley InterScience (www.interscience.wiley.com).

ABSTRACT: Well-defined amphiphilic PCL-*b*-$(PDMA)_2$ and $(PCL)_2$-*b*-PDMA Y-shaped miktoarm star copolymers and PCL-*b*-PDMA linear diblock copolymer were synthesized via a combination of ring-opening polymerization (ROP) and atom transfer radical polymerization (ATRP), where PCL is poly (ε-caprolactone) and PDMA is poly(2-(dimethylamino)ethyl methacrylate). All of these three types of copolymers have comparable PCL contents and overall molecular weights. The PCL block is hydrophobic while the PDMA block is hydrophilic, and they behave like polymeric surfactants and self-assemble into PCL-core micelles in aqueous media. The chain architectural effects on the micellization properties, including the aggregation number, size, polydispersity, and micelle densities of $(PCL_{29})_2$-*b*-$PDMA_{45}$, PCL_{61}-*b*-$(PDMA_{24})_2$, and PCL_{56}-*b*-$PDMA_{49}$ in dilute aqueous solution, were then explored by dynamic and static laser light scattering (LLS). The intensity–average hydrodynamic radius, $\langle R_h \rangle$, the aggregation number per micelle, N_{agg}, and the core radius, R_{core}, of the PCL-core micelles all increased in the order PCL_{61}-*b*-$(PDMA_{24})_2 < (PCL_{29})_2$-*b*-$PDMA_{45} < PCL_{56}$-*b*-$PDMA_{49}$. The surface area occupied per soluble PDMA block at the core/corona interface increased in the order PCL_{61}-*b*-$(PDMA_{24})_2 < PCL_{56}$-*b*-$PDMA_{49} < (PCL_{29})_2$-*b*-$PDMA_{45}$. PCL_{61}-*b*-$(PDMA_{24})_2$ micelles had the largest overall micelle density, possibly because of that the presence of two soluble PDMA arms at the junction point favors the bending of the core–corona interface and thus the formation of densely-packed core-shell nanostructures.
 J Polym Sci Part A: Polym Chem 45: 1446–1462, 2007
Keywords: atom transfer radical polymerization (ATRP); block copolymers; micelles; ring-opening polymerization

INTRODUCTION

The micellar self-assembly of amphiphilic block copolymers in aqueous media is of considerable academic interests due to their diverse applications.[1–6] Structural parameters of amphiphilic block copolymer micelles such as critical micelle concentration (CMC), micelle aggregation number (N_{agg}), average hydrodynamic radius ($\langle R_h \rangle$), micelle shape, and colloidal stability are mainly determined by the solution conditions (pH, temper-

Correspondence to: S. Liu (E-mail: sliu@ustc.edu.cn)
Journal of Polymer Science: Part A: Polymer Chemistry, Vol. 45, 1446–1462 (2007)

ature, and ionic strength), relative block lengths (composition), and molecular weights.[1–9] Recent results have suggested that the block copolymer chain architectures[10] (linear or nonlinear) also play an important role in determining the self-assembly behavior in solution[11–22] or in the condensed state.[23–28] Research focus in this direction has been driven by the concept that the presence of a branching point can reduce the conformational entropy and lead to self-assembled nanostructures different from those observed from their linear counterparts.[11,12,29]

Miktoarm star copolymers (ABC or AB_n, $n \geq 2$) belong to an important category of nonlinear block copolymers, the syntheses of which have been extensively explored.[6,11,12,30–43] Various synthetic techniques such as high vacuum anionic polymerization,[36,44] atom transfer radical polymerization (ATRP),[14,15,24] reversible addition-fragmentation chain transfer (RAFT),[30,37,45] ring-opening polymerization (ROP),[46] nitroxide-mediated radical polymerization (NMP),[35,47] or a combination of them[34,35,38–41,43,48–56] have been successfully developed. However, studies of the self-assembly behavior of miktoarm star copolymers in selective solvents are still quite limited.[14,15,20,34,39–41,57–59]

Pispas et al.[20] studied the micellization properties of PS-*b*-$(PI)_2$, $(PS)_2$-*b*-PI, and PS-*b*-PI copolymers, where PS is polystyrene and PI is polyisoprene. In *n*-decane, a selective solvent for the PI block, the aggregation number, and size of the PS-core micelles increased in the order PS-*b*-$(PI)_2$ < $(PS)_2$-*b*-PI < PS-*b*-PI. They have also developed a simple scaling theory, considering the free energy contributions from the core, the corona, and the interfacial region of the micelles formed from block copolymers with different chain architectures.

Recently, Zubarev and coworkers[40–42] described the synthesis and self-assembly of star-like, V-shaped, and heteroarm star copolymers composed of polybutadiene (PB) and poly(ethylene oxide) (PEO). Armes and coworkers[14,15] reported the preparation of stimulus-responsive Y-shaped double hydrophilic block copolymers, which can self-assemble into micelles with different dimensions compared to those formed by the linear diblock copolymer. However, a detailed comparison of the micellar properties of the amphiphilic Y-shaped AB_2 and A_2B miktoarm star copolymer with that of the linear AB diblock copolymer with comparable composition and molecular weight is still lacking.

If amphiphilic block copolymer micelles were attempted for practical applications such as solubilization of hydrophobic substances and drug delivery, the biodegradability and biocompatibility of the polymeric building blocks are of crucial importance. Poly(ε-caprolactone) (PCL) is an important class of synthetic aliphatic polyester made by the ROP of ε-caprolactone (CL), it is both biocompatible and biodegradable due to the enzymatic and pH dependent cleavage of the ester bonds.[60] On the other hand, poly(2-(dimethylamino)ethyl methacrylate) (PDMA) is a cationic polyelectrolyte at neutral pH and water-soluble over a wide pH range.[61] It can form polyelectrolyte complexes with DNA and is currently under intensive investigation as synthetic vectors for gene delivery.[62–64] Recently, Jakubowski and Matyjaszewski[65] and Mespouille et al.[66] reported the syntheses of poly(ε-caprolactone)-*b*-poly(*n*-octadecyl methacrylate-*co*-2-(dimethylamino)ethyl methacrylate) [PCL-*b*-(PODMA-*co*-PDMA)] and PDMA-*g*-PCL via a combination of ROP and ATRP. To the best of our knowledge, linear and nonlinear shaped amphiphilic block copolymers consisting of PCL and PDMA building blocks have not been reported yet.

In light of these considerations, herein, we describe the synthesis of well-defined amphiphilic Y-shaped A_2B and AB_2 miktoarm star copolymers, $(PCL)_2$-*b*-PDMA and PCL-*b*-$(PDMA)_2$. The synthesis was accomplished by a combination of ROP and ATRP using two types of trifunctional initiators, Br_m-Init-$(OH)_n$ ($m = 2$, $n = 1$; $m = 1$, $n = 2$). For comparison, PCL-*b*-PDMA linear diblock copolymer with similar composition and overall molecular weight to the miktoarm star copolymers was also prepared. The chain architectural effects on the micellization properties, including the aggregation number, size, polydispersity, and micelle densities of $(PCL)_2$-*b*-PDMA, PCL-*b*-$(PDMA)_2$, and PCL-*b*-PDMA in dilute aqueous solution were explored by dynamic and static laser light scattering (LLS).

EXPERIMENTAL

Materials

2-Hydroxyethyl acrylate (HEA, 95%, Aldrich) was passed through an alumina column to remove the inhibitor. 2-(Dimethylamino)ethyl methacrylate (DMA, Aldrich) was vacuum distilled from CaH_2. All monomers were stored in a refrigerator before use. ε-Caprolactone (CL, 99%, Acros) was dried over CaH_2 for 48 h and then distilled under high vacuum just prior to use. Tetrahydrofuran (THF) were dried by refluxing over sodium/benzophenone and distilled prior to use. Triethylamine (TEA),

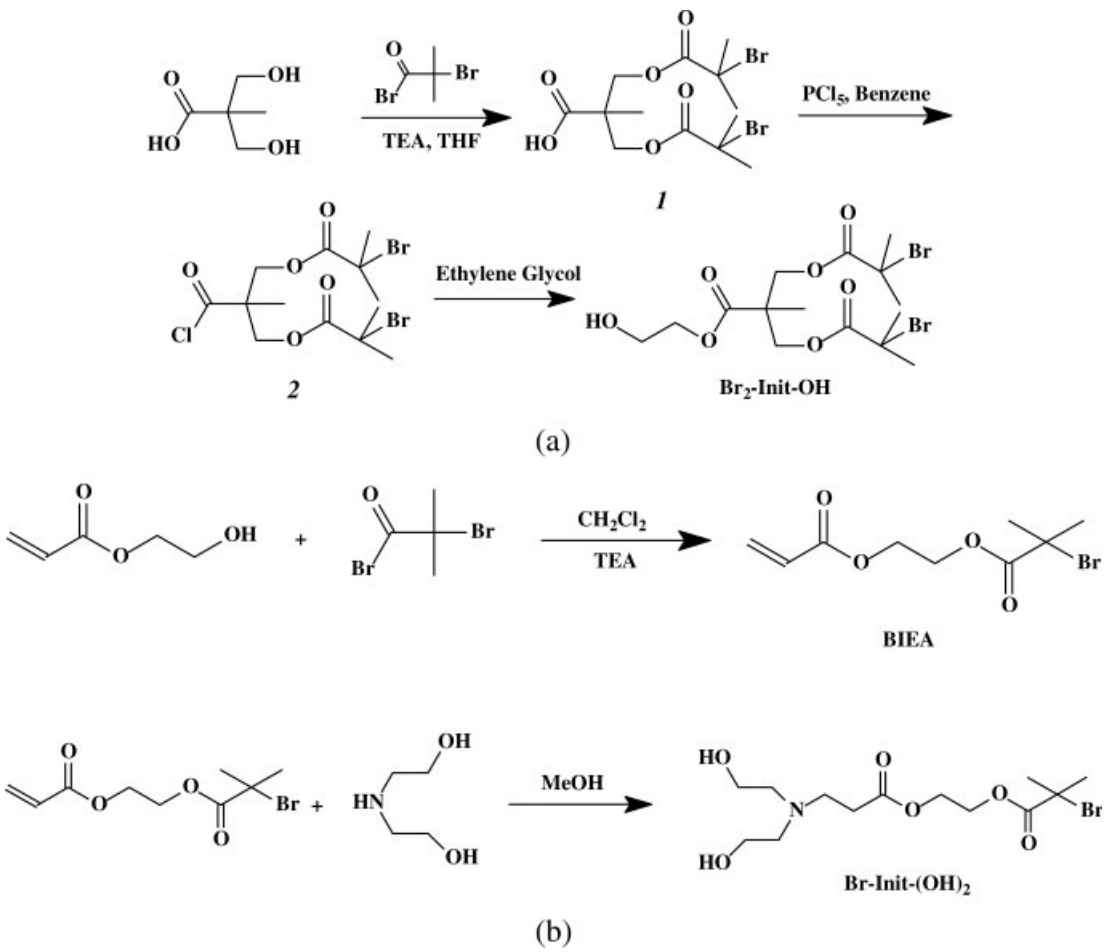

Scheme 1. Synthetic routes for the trifunctional initiators: (a) Br_2-Init-OH and (b) Br-Init-$(OH)_2$.

ethylene glycol (EG), dichloromethane (CH_2Cl_2), methanol (MeOH), and *N,N*-dimethylformamide (DMF) were dried over CaH_2 and distilled at reduced pressure. 2-Bromoisobutyryl bromide (98%, Aldrich), copper(I) bromide (CuBr, 98%, Aldrich), 2,2′-bipyridine (bpy, 99+%, Aldrich), tin(II) 2-ethylhexanoate ($Sn(Oct)_2$, 95%, Sigma), and other reagents were used as received.

Synthesis

The general synthetic routes for the preparation of the trifunctional initiators, Br-Init-$(OH)_2$ and Br_2-Init-OH, and the Y-shaped miktoarm star copolymers, $(PCL)_2$-*b*-PDMA and PCL-*b*-$(PDMA)_2$, were shown in Schemes 1 and 2, respectively.

Synthesis of Trifunctional Initiator Br-Init-$(OH)_2$ (Scheme 1)[14]

HEA (20 mL, 174.1 mmol), anhydrous CH_2Cl_2 (200 mL), and TEA (27 mL, 193.6 mmol) were added to a dry 500-mL round-bottomed flask. 2-Bromoisobutyryl bromide (24 mL, 194.2 mmol) was added dropwise to the ice-cooled flask via syringe over 30 min under stirring. The mixture was stirred at 0 °C for 1 h and then at room temperature for 8 h. The resulting reaction mixture was filtered to remove the insoluble salt and then washed three times with saturated aqueous solution of $NaHCO_3$ (100 mL each). The organic layer was collected and dried over anhydrous $MgSO_4$, then passed through a silica column using CH_2Cl_2 as an eluent. The solvent was removed under reduced pressure to afford acryloyloxyethyl 2-bromoisobutyrate (BIEA) as a light yellow liquid (40 g, yield: 87%). ^{1}H NMR ($CDCl_3$, δ): 6.47–5.85 (3H, CH_2=CHCOO), 4.42 (4H, COOCH_2CH_2OCO), 1.93 (6H, C(CH_3)$_2$Br).

Diethanolamine (4.66 g, 44.3 mmol), anhydrous MeOH (20 mL), and 10 mg hydroquinone were added to a 100-mL flask and immersed into an ice bath under stirring. BIEA (9.6 g, 36.2 mmol) was added dropwise to the flask over 1 h. Then the mix-

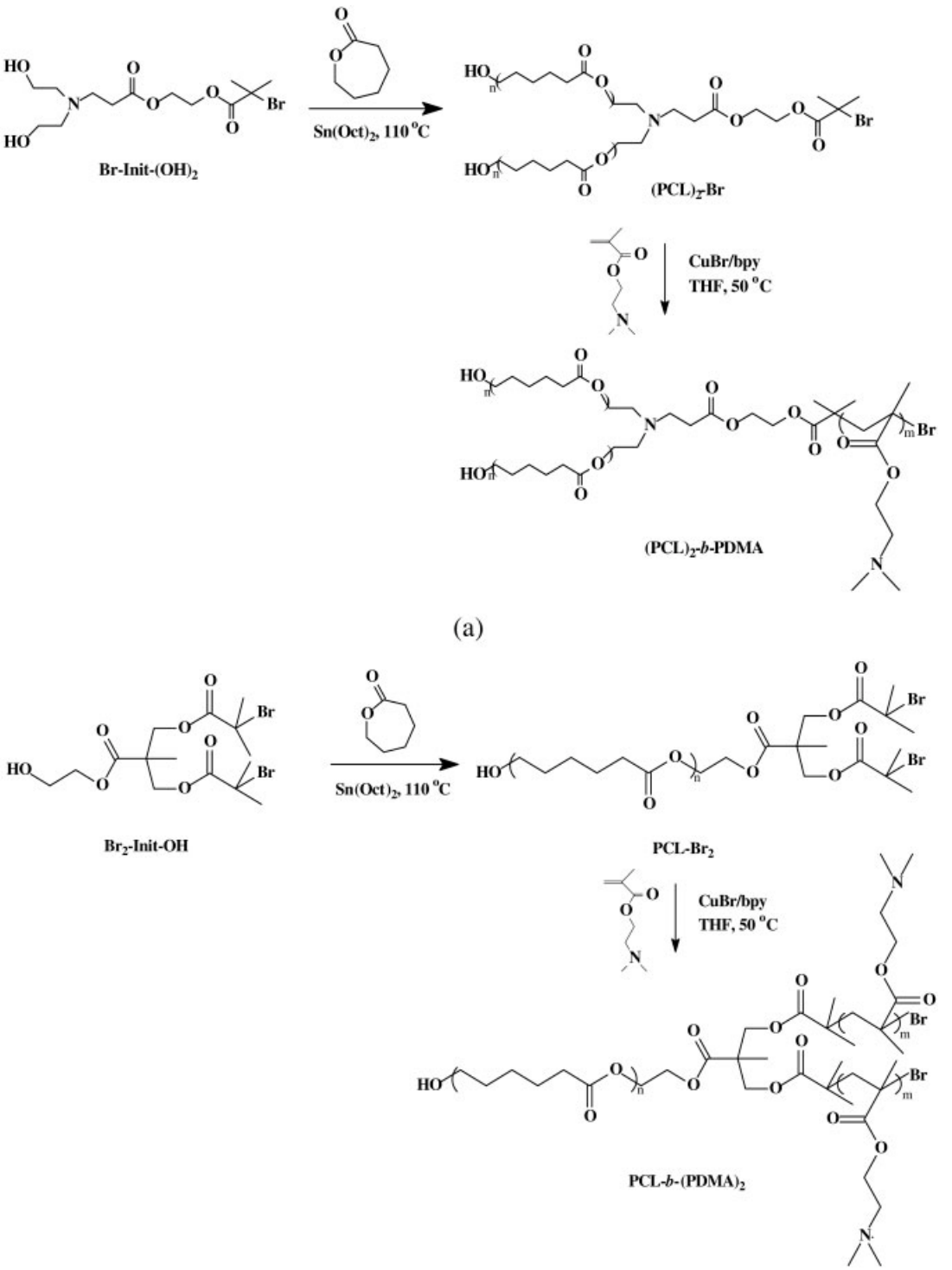

Scheme 2. Synthetic routes for (a) $(PCL)_2$-*b*-PDMA and (b) PCL-*b*-$(PDMA)_2$ Y-shaped miktoarm star copolymers by a combination of the ROP of CL and the ATRP polymerization of DMA.

ture was stirred at room temperature for 8 h. The resulting reaction mixture was extracted using toluene and *n*-hexane, followed by passing through a silica gel column using THF/CH_2Cl_2 = 1:1 as an eluent to remove residual reactants. Solvents were removed under reduced pressure to afford a light yellow liquid, Br-Init-$(OH)_2$ (7.2 g, yield: 50%). ^{1}H NMR ($CDCl_3$, δ): 4.38 (4H, COOCH_2CH_2OCO), 3.61 (4H, CH_2OH), 2.53 (2H, OOCCH_2), 2.65 (4H, CH_2N(CH_2)$_2$), 2.87 (2H, CH_2N(CH_2)$_2$), 1.94 (6H, C(CH_3)$_2$Br).

Synthesis of Trifunctional Initiator Br_2-Init-OH (Scheme 1)[56]

In a three-neck flask equipped with a magnetic stirrer, 2, 2-bis(hydroxymethyl)propionic acid (5 g, 37 mmol) was dissolved in anhydrous THF (80 mL). TEA (12.6 mL, 90 mmol) was added and the solution became homogeneous. The flask was ice-cooled to 0 °C. A solution of 2-bromoisobutyryl bromide (11.1 mL, 90 mmol) in THF was added through a dropping funnel. The mixture was kept under stirring at room temperature overnight. The salt was filtered off and the solvent was completely removed under vacuum. A pale yellow viscous liquid (**1**) was obtained (15 g, yield: 94%) and used without further purification. Compound **1** (4.32 g, 10 mmol) was dissolved in benzene (50 mL). Phosphorus pentachloride (PCl_5, 7.5 g, 36 mmol) was then added. The mixture turned immediately to orange color; the solution was kept under stirring at room temperature overnight. Then the insoluble salt was filtered off and benzene was removed under reduced pressure. Hexane was added to remove the excess PCl_5. The organic phase was recovered and the solvent evaporated under vacuum. A clearly brown liquid (**2**) was obtained (4.47 g, yield: 99%). ^{1}H NMR ($CDCl_3$, δ): 4.43 (s, 4H, *C*H_2 OCO), 1.92 (s, 12H, —(*C*H_3)$_2$CBr), 1.48 (s, 3H, *C*H_3).

Compound **2** (4.47 g, 10 mmol) was then added to a molar excess (25 times) of EG (17.3 mL), and the mixture was reacted for 24 h in a Schlenk tube, which was cooled to 0 °C. The reaction mixture was dissolved in water and extracted with CH_2Cl_2. The organic phase was successively washed with saturated aqueous solution of $NaHCO_3$ and water, and then dried over anhydrous $MgSO_4$. The solvent was removed under reduced pressure, and Br_2-Init-OH was collected as orange oil without further purification (4.1 g, yield: 86%). ^{1}H NMR ($CDCl_3$, δ): 4.47–4.35 (4H, —C(CH_3)CH_2OCO), 4.28 (2H, HOCH_2CH_2OCO), 3.84 (2H, HOCH_2 CH_2OCO), 2.12 (1H, *H*OCH_2), 1.92 [12H, C(CH_3)$_2$Br], 1.37 (3H, —CCH_3).

Synthesis of PCL-Based ATRP Macroinitiators by ROP (Scheme 2)

The PCL macroinitiators $(PCL)_2$-Br and PCL-Br_2 were prepared via the ROP of CL monomer catalyzed by $Sn(Oct)_2$ in bulk at 110 °C for 24 h with Br-Init-$(OH)_2$ and Br_2-Init-(OH) as initiators, respectively. To a previously flamed Schlenk tube equipped with a magnetic stirring bar, the initiator and a solution of catalyst in toluene (0.1 mol/L) were added, then toluene was evaporated under vacuum and CL were added subsequently. The tube was carefully degassed by three freeze-thaw cycles, sealed under vacuum, and placed in a thermostated oil bath at 110 °C. The resulting reaction mixture was dissolved in THF, precipitated into a large excess of methanol, and then isolated by vacuum filtration. The product was then dried *in vacuo* at room temperature overnight. The experimental conditions of the ROP polymerization were summarized in Table 1.

Synthesis of Miktoarm Star Copolymers by ATRP (Scheme 2)

The synthesis of the $(PCL)_2$-*b*-PDMA and PCL-*b*-$(PDMA)_2$ miktoarm star copolymers was accomplished by the ATRP polymerization of DMA using CuBr/bpy as the catalyst. $(PCL)_2$-Br and PCL-Br_2 were employed as initiators for the preparation of $(PCL)_2$-*b*-PDMA and PCL-*b*-$(PDMA)_2$, respectively. The details for the polymerization conditions are summarized in Table 1. The polymerization was carried out at 50 °C in THF under degassed conditions for 12 h. After the polymerization, the reaction mixture was diluted with THF and then passed through a column of neutral alumina for the removal of copper catalysts. The solvent and unreacted DMA monomers were removed under reduced pressure. The resulting product was dissolved in THF and precipitated into *n*-hexane, and this cycle was repeated twice. The product was dried *in vacuo* at room temperature overnight.

Synthesis of PCL-*b*-PDMA Linear Diblock Copolymer by ROP and ATRP

The initiator 2-hydroxyethyl 2′-bromoisobutyrate, Br-Init-(OH), was prepared by the esterification reaction of 2-bromoisobutyryl bromide with excess

Table 1. Summary of the Synthetic Conditions and Molecular Parameters of Y-Shaped Miktoarm Star and Linear Diblock Copolymers and the PCL-Based ATRP Macroinitiators

Samples	Initiator	Monomer	Catalysts	$[M]^0$ (mol/L)	$[M]^0$:[initiator]:[catalyst]	$M_{n,cal}$[a]	DP of PCL[b]	DP of PDMA[c]	wt_{PCL} (%)	$M_{n,NMR}$	M_w/M_n[d]
$(PCL)_2$-Br[e]	Br-Init-$(OH)_2$	CL	$Sn(Oct)_2$	9.02	60:1:0.08	7,200	29	/	/	6,900	1.21
$(PCL)_2$-*b*-PDMA[f]	PCL_2-Br	DMA	CuBr/bPy	2.49	50:1:1:2	14,300	29	45	48	14,000	1.13
PCL-Br_2[e]	Br_2-Init-OH	CL	$Sn(Oct)_2$	9.02	60:1:0.04	7,300	61	/	/	7,400	1.09
PCL-*b*-$(PDMA)_2$[f]	PCL-Br_2	DMA	CuBr/bPy	2.49	50:1:1:2	15,400	61	24	48	14,900	1.14
PCL-Br[a]	Br-Init-(OH)	CL	$Sn(Oct)_2$	9.02	60:1:0.04	7,000	56	/	/	6,500	1.37[g]
PCL-*b*-PDMA[f]	PCL-Br	DMA	CuBr/bPy	2.49	50:1:1:2	14,400	56	49	45	14,300	1.19[g]

[a] The theoretical molecular weights were calculated as: $M_{n,cal} = MW_{initiator} + MW_{monomer} \times DP_{n,target}$, $DP_{n,target} = [M]^0/[initiator] \times$ conversion.
[b] Determined by ^{1}H NMR for the PCL block of PCL-*b*-$(PDMA)_2$ and PCL-*b*-PDMA, or one PCL arm of $(PCL)_2$-*b*-PDMA.
[c] Determined by ^{1}H NMR for the PDMA block of $(PCL)_2$-*b*-PDMA and PCL-*b*-PDMA, or one PDMA arm of PCL-*b*-$(PDMA)_2$.
[d] Determined by GPC in DMF at a flow rate of 1.0 mL/min.
[e] The polymerization conditions: bulk, 110 °C, 24 h.
[f] The polymerization conditions: THF, 50 °C, 12 h.
[g] The eluent was THF at a flow rate of 1.0 mL/min.

EG, following literature procedures.[67] The linear PCL-*b*-PDMA block copolymer was synthesized according to similar procedures as described earlier (Table 1).

Preparation of Micellar Solutions

Ten milligrams $(PCL)_2$-*b*-PDMA, PCL-*b*-$(PDMA)_2$, or PCL-*b*-PDMA was dissolved in 2 mL DMF. Eighteen millilitres deionized water was added slowly (~1 mL/min) under vigorous stirring, the mixture was left stirring for an additional 12 h. DMF was then removed by dialysis against deionized water for 2 days. Stock solutions with a characteristic bluish tinge were typically obtained, suggesting the formation of PCL-core micelles. The micellar solution exhibited no macroscopic phase separation upon standing at room temperature for several weeks.

Characterization

Nuclear Magnetic Resonance (NMR) Spectroscopy

All ^{1}H-NMR spectra were recorded at 27 °C on a Bruker AV300 NMR spectrometer (resonance frequency of 300 MHz for ^{1}H and 75 MHz for ^{13}C) operated in the Fourier transform mode. $CDCl_3$ was used as the solvent.

Gel Permeation Chromatograph (GPC)

Molecular weight distributions were determined by GPC using a series of two linear Styragel columns HT3, HT4, and an oven temperature of 60 °C. Waters 1515 pump and Waters 2414 differential refractive index detector (set at 30 °C) were used. The eluent was DMF + 1 g/L LiBr at a flow rate of 1.0 mL/min. A series of six polystyrene standards with molecular weights ranging from 800 to 400,000 g/mol were used for calibration.

Laser Light Scattering (LLS)

A commercial spectrometer (ALV/DLS/SLS-5022F) equipped with a multi-tau digital time correlator (ALV5000) and a cylindrical 22 mW Uniphase He-Ne laser (λ_0 = 632 nm) as the light source was used. In static LLS (SLS), we can obtain the weight–average molar mass (M_w) and the *z*-average root-mean square radius of gyration ($\langle R_g^2 \rangle^{1/2}$ or written as $\langle R_g \rangle$) of polymer chains in a dilute solution from the angular dependence of the excess

absolute scattering intensity, known as Rayleigh ratio $R_{vv}(q)$, as

$$\frac{KC}{R_{vv}(q)} \approx \frac{1}{M_w}\left(1 + \frac{1}{3}\langle R_g^2\rangle q^2\right) + 2A_2C \qquad (1)$$

where $K = 4\pi^2 n^2 (dn/dC)^2/(N_A\lambda_0^4)$ and $q = (4\pi n/\lambda_0)\sin(\theta/2)$ with N_A, dn/dC, n, and λ_0 being the Avogadro number, the specific refractive index increment, the solvent refractive index, and the wavelength of the laser light in a vacuum, respectively; and A_2 is the second virial coefficient. dn/dC was determined using an Optokem differential refractometer operating at 632.8 nm. Strictly speaking, here $R_{vv}(q)$ should be $R_{vu}(q)$ because there is no analyzer before the detector. However, the depolarized scattering of the solution studied is insignificant so that $R_{vu}(q) \sim R_{vv}(q)$. Also note that in this study, the sample solution was so dilute (0.1 g/L) that the extrapolation of $C \rightarrow 0$ was not necessary, and the term $2A_2C$ in eq 1 can be neglected.

In dynamic LLS (DLS), the Laplace inversion of each measured intensity–intensity-time correlation function $G^{(2)}(q,t)$ in the self-beating mode can lead to a line-width distribution $G(\Gamma)$. For a pure diffusive relaxation, Γ is related to the translational diffusion coefficient D by $(\Gamma/q^2)_{C\rightarrow 0, q\rightarrow 0} \rightarrow D$, or further to the hydrodynamic radius R_h via the Stokes–Einstein equation, $R_h = (k_BT/6\pi\eta_0)/D$, where k_B, T, and η_0 are the Boltzmann constant, the absolute temperature, and the solvent viscosity, respectively.

Transmission Electron Microscopy (TEM)

TEM observations were conducted on a Hitachi H-800 electron microscope at an acceleration voltage of 200 kV. The sample for TEM observations was prepared by placing a light drop of solution on copper grids coated with thin films of Formvar and carbon successively, then stained with $RuCl_4$.

RESULTS AND DISCUSSION

Several groups reported the syntheses of nonlinear-shaped block copolymers, including AB_2 miktoarm star,[38,56,68] ABC miktoarm star,[54] H-shaped,[69,70] π-shaped,[71] and dendrimer-like star copolymers[43,72,73] via the combination of ROP and ATRP techniques. Multifunctional initiators with hydroxyl and bromine terminal groups were typically employed for the initiation of ROP and ATRP polymerizations, respectively. In this study, we follow similar principles in synthesizing the Y-shaped $(PCL)_2$-*b*-PDMA and PCL-*b*-$(PDMA)_2$, and the linear PCL-*b*-PDMA copolymers. Moreover, we focused on preparing nonlinear amphiphilic (A_2B, AB_2) and linear (AB) block copolymers with comparable compositions and molecular weights, which made it possible to study the chain architectural effects on the micellization properties in aqueous media. The general synthetic routes used for the 3-step preparation of Y-shaped $(PCL)_2$-*b*-PDMA and PCL-*b*-$(PDMA)_2$ miktoarm star copolymers were shown in Schemes 1 and 2. The first step involved is the preparation of well-defined trifunctional initiators, Br-Init-$(OH)_2$ and Br_2-Init-OH, with hydroxyl and bromine terminal end groups, following literature procedures reported by Armes and coworkers[14,15] and Tunca and coworkers,[56] with slight modifications. This was followed by the ROP of CL, yielding ATRP macroinitiators, $(PCL)_2$-Br and PCL-Br_2 (Scheme 2). $(PCL)_2$-*b*-PDMA and PCL-*b*-$(PDMA)_2$ were then obtained by the ATRP of DMA monomers using $(PCL)_2$-Br and PCL-Br_2 as macroinitiators.

Syntheses of Trifunctional Initiators

During the preparation of Br-Init-$(OH)_2$ (Scheme 1b), ^{1}H NMR studies indicated that the esterification reaction of HEA using excess 2-bromoisobutyryl bromide was essentially complete, and the characteristic signals of HEA at $\delta = 3.8$ ppm (CH_2OH) totally disappeared after esterification. The presence of a single peak at $\delta = 1.94$ ppm indicated that the excess 2-bromoisobutyryl bromide was completely removed. Peak integrals (see Experimental Section) were consistent with the target compound, acryloyloxyethyl 2-bromoisobutyrate (BIEA). The trifunctional initiator, Br-Init-$(OH)_2$, was subsequently obtained via the Michael addition of BIEA with a 20% excess of diethanolamine.[14] The reaction temperature was controlled at 0 °C initially because lower temperature was favorable for Michael addition and unfavorable for the side reactions (e.g., polymerization and the hydroxyl addition to the double bonds).[74] We found that the addition of hydroquinone as an inhibitor was necessary and longer reaction time (>12 h) lead to unwanted side products. After stirring for 8 h at room temperature, no residual acryloyl signals could be discerned at $\delta = 6.47$–5.85 ppm in the ^{1}H NMR spectrum, indicating that the reaction went to completion.

The trifunctional initiator Br_2-Init-OH was prepared from 2,2-bis(hydroxymethyl)- propionic acid via three-step reactions.[56] After esterification with 2-bromoisobutyryl bromide, the signals at $\delta = 3.5$ ppm for methylene protons next to the hydroxyl group in the starting material completely disap-

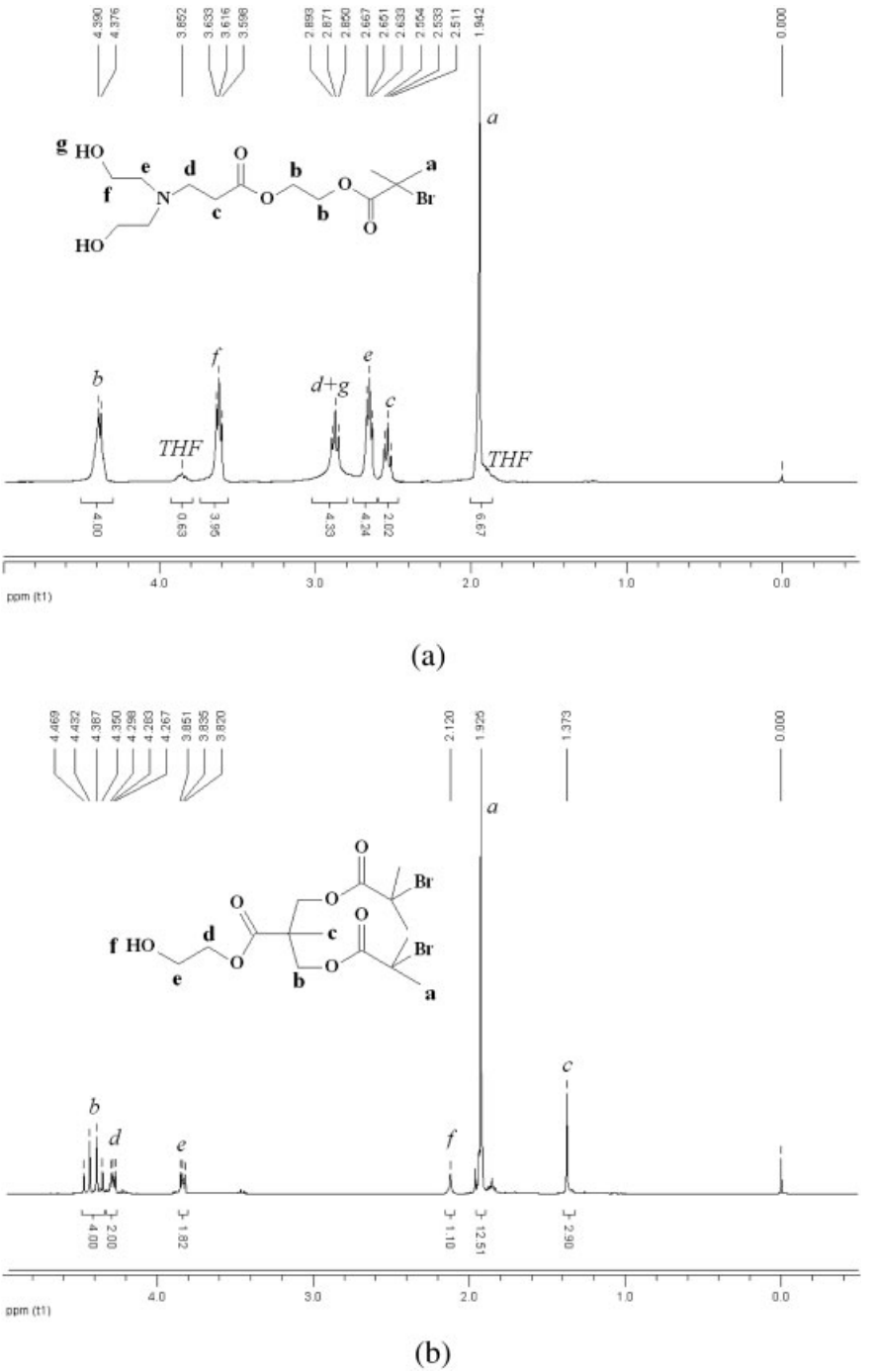

Figure 1. ^{1}H NMR spectra of the trifunctional initiators Br-Init-$(OH)_2$ (a) and Br_2-Init-OH (b) in $CDCl_3$.

peared. ^{1}H NMR spectrum of Br_2-Init-OH [Fig. 1(b)] revealed that the resonance of $HOCH_2CH_2$ was located at 3.84 ppm. Peak integral ratios were consistent with the target compound, Br_2-Init-OH.

^{13}C-NMR spectra of the trifunctional initiators, Br-Init-$(OH)_2$ and Br_2-Init-OH, are shown in Figure 2, in which the respective resonances were clearly assigned and consistent with the target compounds.

The experimental conditions and the molecular parameters of the prepared PCL-based macroinitiators and Y-shaped $(PCL)_2$-*b*-PDMA and PCL-*b*-$(PDMA)_2$ miktoarm star copolymers are summarized in Table 1.

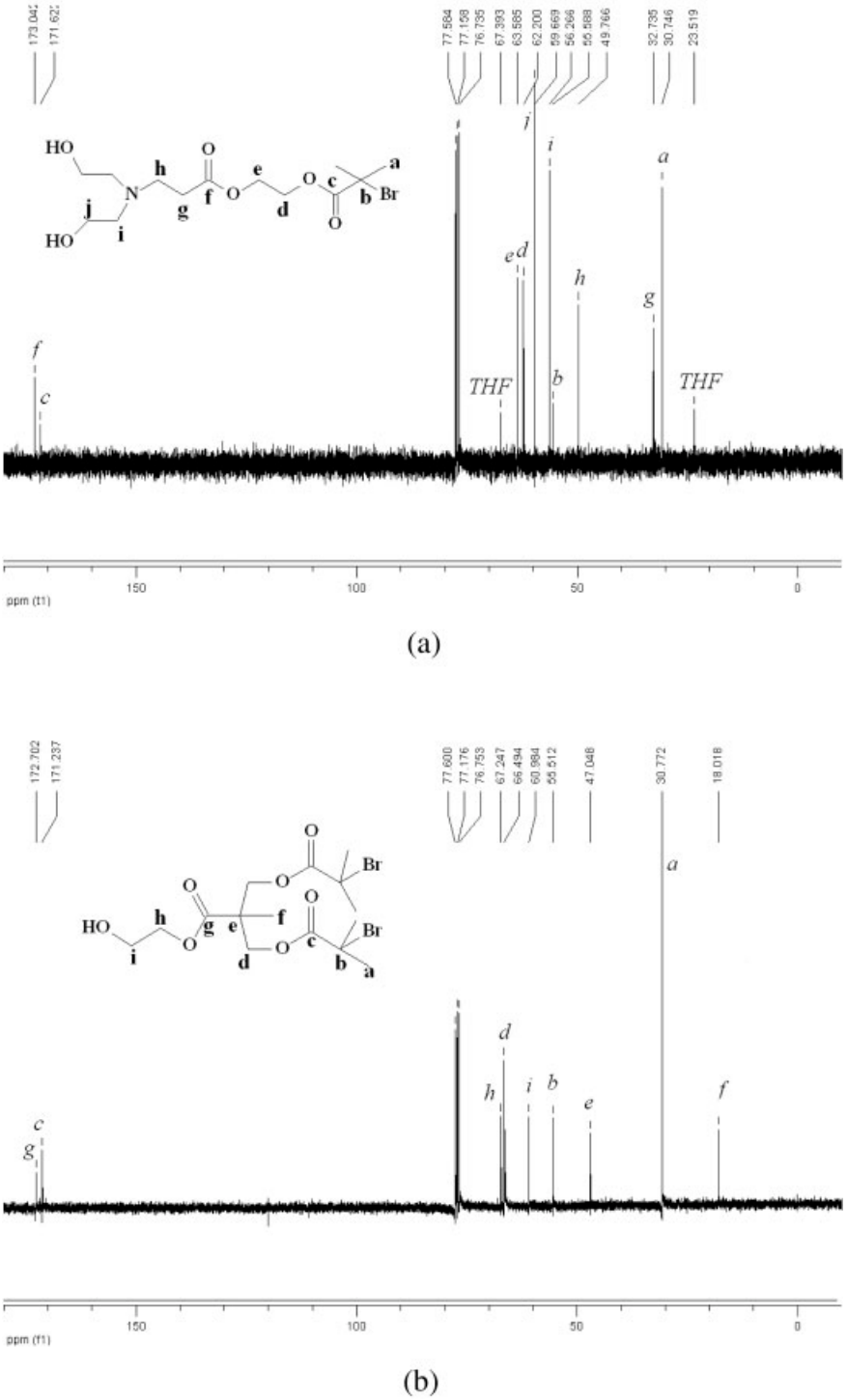

Figure 2. ^{13}C NMR spectra of the trifunctional initiators Br-Init-$(OH)_2$ (a) and Br_2-Init-OH (b) in $CDCl_3$.

Synthesis of PCL-Based ATRP Macroinitiators by ROP

The PCL-based ATRP macroinitiators containing single or dual bromine end groups were prepared by the ROP of CL in bulk at 110 °C using Br-Init-$(OH)_2$ and Br_2-Init-OH as initiators and $Sn(Oct)_2$ as the catalyst. The conversion typically went to nearly 100% after 24 h under our conditions.[75] ^1H

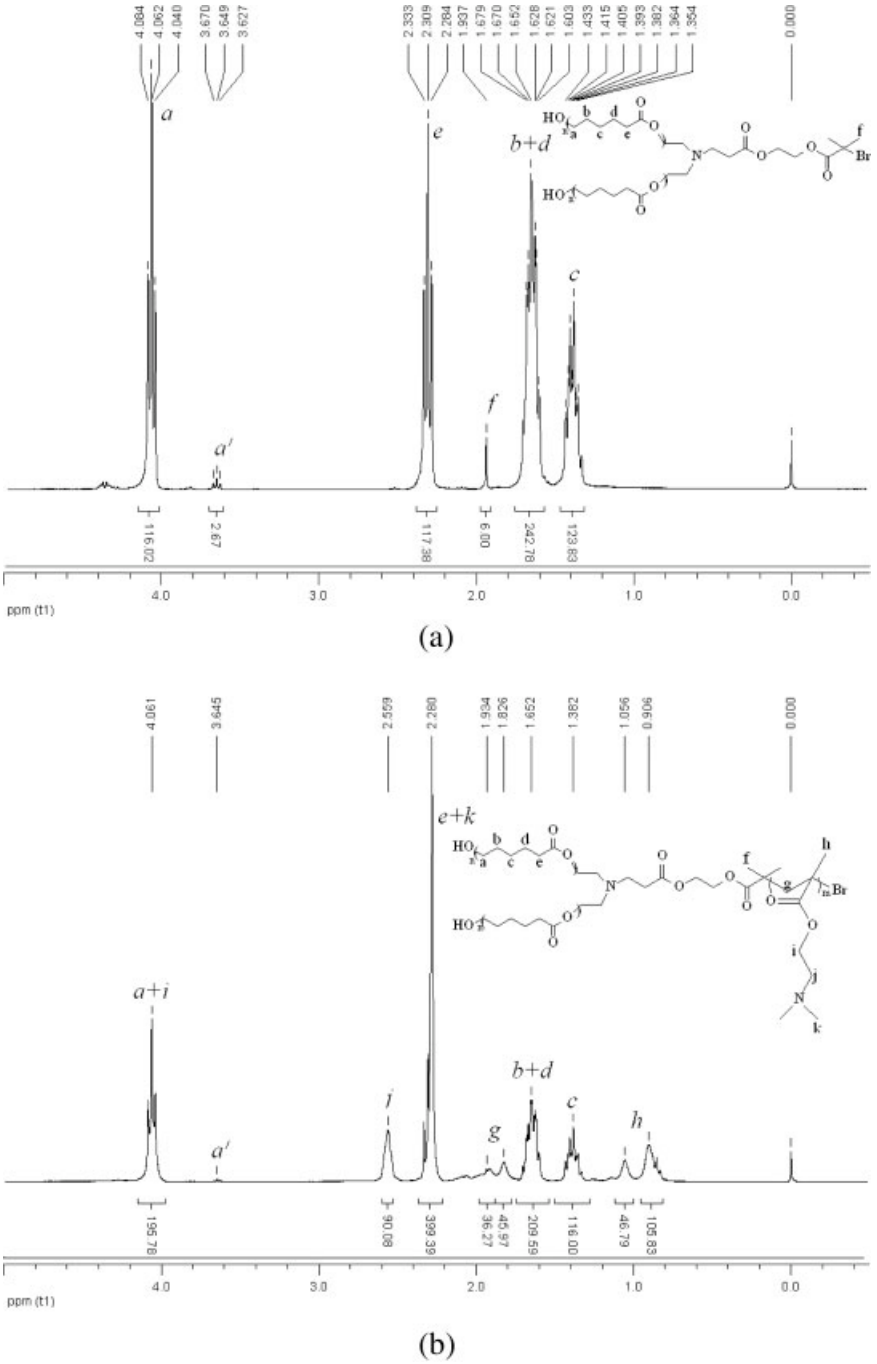

Figure 3. ^{1}H NMR spectra of (a) $(PCL_{29})_2$-Br precursor and (b) $(PCL_{29})_2$-*b*-$PDMA_{45}$ Y-shaped miktoarm star copolymer in $CDCl_3$.

NMR spectra of the PCL-based macroinitiators are shown in Figures 3 and 4, in which the respective resonances, including the bromine end groups, were clearly assigned. The number–average molecular weight of PCL-based macroinitiators calculated from ^{1}H NMR, $M_{n,NMR}$, which was determined from the ratio of the integrated peak areas of the methylene groups ($COOCH_2CH_2CH_2$, 4.1 ppm) in CL units and the 2-bromisobutyrate end groups ($C(CH_3)_2Br$, 1.9 ppm), was in good agreement with the calculated target molecular weights, $M_{n,cal}$ (see Table 1). Typical GPC traces of $(PCL)_2$-Br and $PCL\text{-}Br_2$ are shown in Figures 5 and 6, respectively. Both of them were mono-modal and relatively symmetric. The number–average molecular weights, M_n, were determined to be 6100 and 6300, with poly-

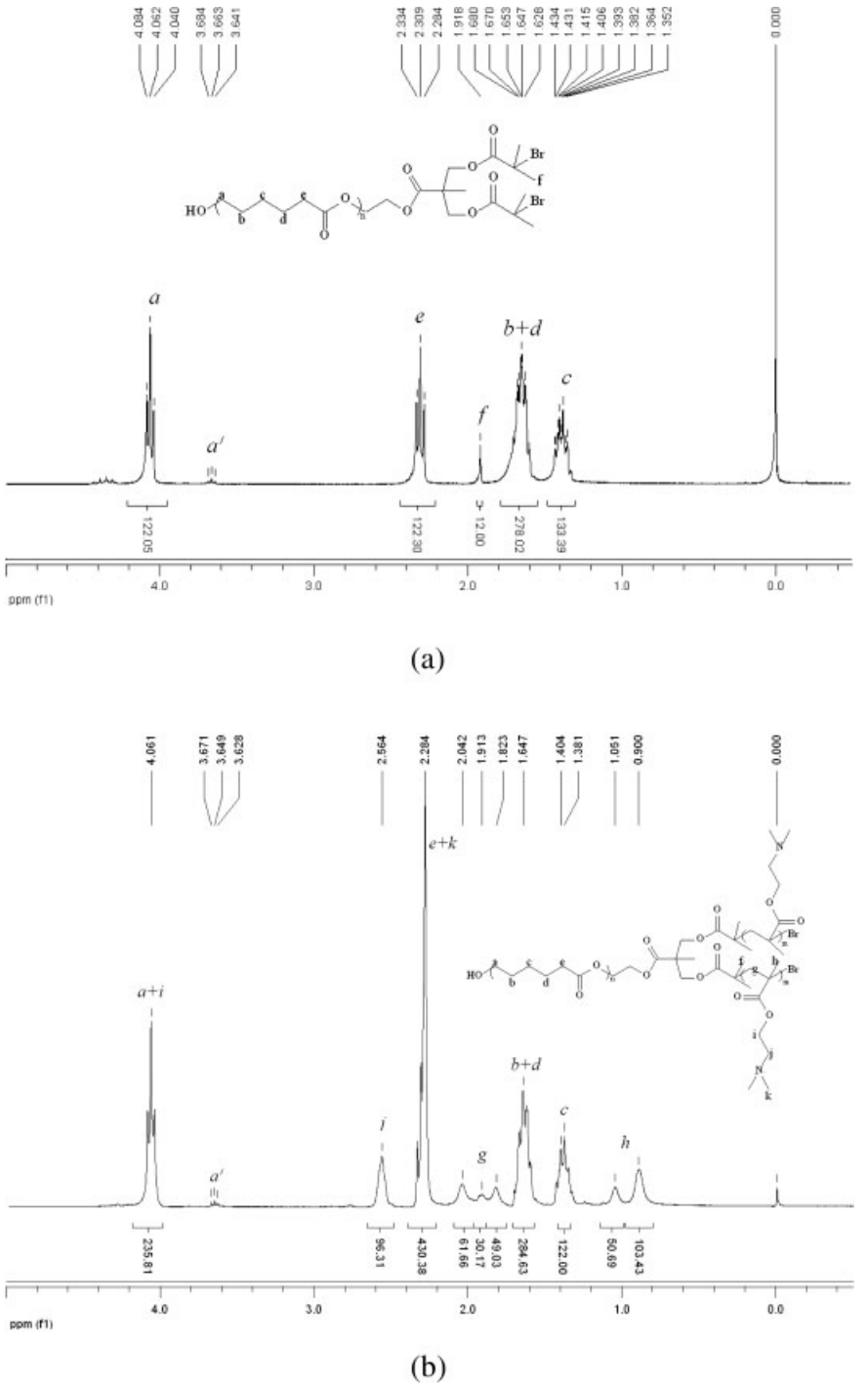

Figure 4. ^{1}H NMR spectra of (a) PCL_{61}-Br_2 precursor and (b) PCL_{61}-*b*-$(PDMA_{24})_2$ Y-shaped miktoarm star copolymer in $CDCl_3$.

dispersity, M_w/M_n, being 1.21 and 1.09 for $(PCL)_2$-Br and PCL-Br_2, respectively. The actual degree of polymerization, DP, of the PCL block was determined from ^{1}H-NMR. The obtained $(PCL_{29})_2$-Br and PCL_{61}-Br_2 were subsequently employed as ATRP macroinitiators for the polymerization of DMA.

Synthesis of Miktoarm Star Copolymers by ATRP

$(PCL_{29})_2$-Br and PCL_{61}-Br_2 were employed as macroinitiators for the ATRP polymerization of DMA in THF at 50 °C using CuBr/bpy complexes as the catalyst (Table 1).[65,76] Typical conversions were

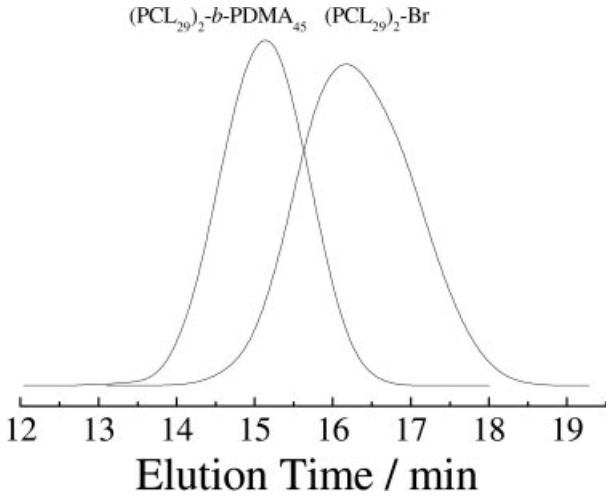

Figure 5. GPC traces of the ATRP macroinitiator, $(PCL_{29})_2$-Br, and the miktoarm star copolymer, $(PCL_{29})_2$-*b*-$PDMA_{45}$.

~90% after 12 h. ^{1}H NMR spectra of $(PCL)_2$-*b*-PDMA and PCL-*b*-$(PDMA)_2$ shown in Figures 3 and 4 revealed that the characteristic NMR resonances of PDMA and PCL were clearly evident, and all signals were assigned. The GPC traces of the prepared $(PCL)_2$-*b*-PDMA and PCL-*b*-$(PDMA)_2$ are shown in Figures 5 and 6, respectively. In both cases, we can observe the clear shift to higher molecular weight after the ATRP polymerization of DMA compared to the PCL-based initiators. It is well-known that for nonlinear block copolymers, GPC analysis tends to underestimate the molecular weight due to reduced hydrodynamic volumes. The actual DP of the PDMA branch of the resulting miktoarm star copolymers was determined from the integral ratio of peaks at $\delta = 2.6$ ppm characteristic of PDMA to that at $\delta = 1.4$ ppm characteristic of PCL. The results are summarized in Table 1.

GPC traces of both $(PCL)_2$-*b*-PDMA and PCL-*b*-$(PDMA)_2$ were mono-modal and quite symmetric, revealing polydispersity of 1.13 and 1.14, and M_n of 11,500 and 12,400, respectively. This indicated that well-defined nonlinear A_2B or AB_2 miktoarm star copolymers were obtained. If the 3-miktoarm star copolymers contained some 2-arm side products, which may occur due to the intramolecular irreversible termination reactions or the inefficient initiation during polymerization, the GPC curve will exhibit a tail at the lower molecular weight side. We can thus at least conclude that the major products were the desired 3-miktoarm star copolymers.[48,56,77]

For comparison, we have also synthesized the PCL_{56}-*b*-$PDMA_{49}$ linear diblock copolymer with similar PCL content and molecular weight to that of the miktoarm star copolymers, following similar procedures as described earlier. Table 1 summarizes the molecular parameters of these three types of copolymers.

Chain Architectural Effects on Micellar Properties

PCL is essentially hydrophobic, whereas PDMA is a weak polybase with a pK_a of ~7.0. At room temperature, PDMA homopolymer is water-soluble over a wide pH range. However, it exhibits inverse temperature solubility behavior and precipitates from neutral or basic aqueous solution between 32 and 53 °C, depending on its molecular weight.[61] In aqueous solution, the amphiphilic Y-shaped PCL_{61}-*b*-$(PDMA_{24})_2$ and $(PCL_{29})_2$-*b*-$PDMA_{45}$ miktoarm star copolymers and the linear PCL_{56}-*b*-$PDMA_{49}$ diblock copolymer will form core-shell nanoparticles, with the core consisting of the insoluble PCL block and the shell being the soluble PDMA block. The formation of PCL-core micelles was evidenced by the appearance of bluish tinge after addition of water into polymer solutions in DMF. It should be noted that during the preparation of micelles, water was slowly added into the polymer solution in DMF. Above the critical water content, the micelle structures were kinetically frozen. We expect that the prepared micelles will not relax into their final equilibrium structures due to the crystallinity of PCL branches. After removing DMF by dialysis, the micellar solutions were further diluted to 0.1 g/L and characterized by a com-

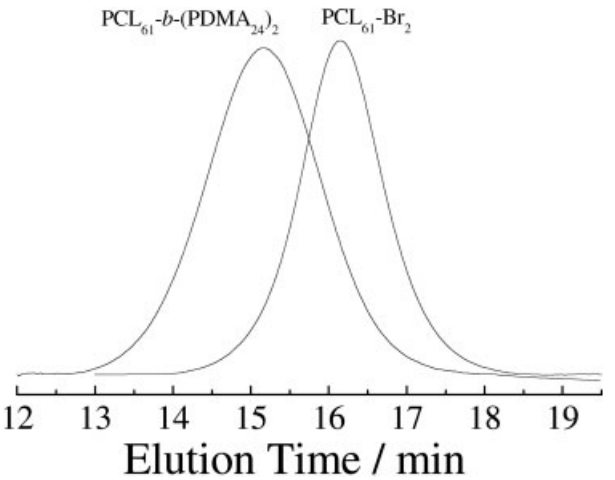

Figure 6. GPC traces of the ATRP macroinitiator, PCL_{61}-Br_2, and the miktoarm star copolymer, PCL_{61}-*b*-$(PDMA_{24})_2$.

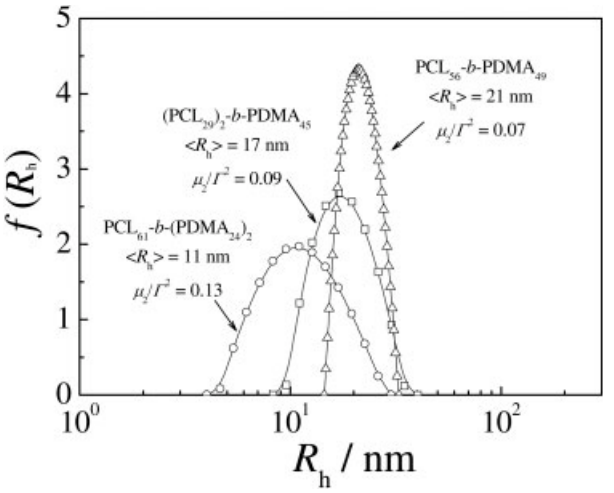

Figure 7. Hydrodynamic radius distributions, $f(R_h)$, of the micelles prepared from $(PCL_{29})_2$-*b*-$PDMA_{45}$, PCL_{61}-*b*-$(PDMA_{24})_2$, and PCL_{56}-*b*-$PDMA_{49}$ in aqueous solution at a concentration of 0.1 g/L.

bination of TEM and laser light scattering at 25 °C.

Figure 7 showed typical hydrodynamic radius distributions, $f(R_h)$, of micellar solutions prepared from PCL_{61}-*b*-$(PDMA_{24})_2$, $(PCL_{29})_2$-*b*-$PDMA_{45}$, and PCL_{56}-*b*-$PDMA_{49}$ at a concentration of 0.1 g/L. Contin analysis revealed the presence of only one type of diffusing species for all the three samples. The polydispersity of the micelles, as evaluated through the ratio μ_2/Γ^2 by cumulants analysis, where μ_2 was the second moment in the cumulant expansion of the correlation function and Γ was the decay rate, were relatively narrow ($\sim$0.1). μ_2/Γ^2 values of the miktoarm star copolymer micelles were slightly larger than that of linear diblock copolymer. In the concentration range 0.01–0.2 g/L, $<R_h>$ of all three types of micelles remained essentially constant, suggesting that their CMC were well below 0.01 g/L.

The average hydrodynamic radius, $<R_h>$, increased in the order PCL_{61}-*b*-$(PDMA_{24})_2$ < $(PCL_{29})_2$-*b*-$PDMA_{45}$ < PCL_{56}-*b*-$PDMA_{49}$. The apparent weight–average molecular weight, $M_{w,app}$, of PCL_{56}-*b*-$PDMA_{49}$ micelles is much larger than that of $(PCL_{29})_2$-*b*-$PDMA_{45}$ and PCL_{61}-*b*-$(PDMA_{24})_2$. The aggregation number, N_{agg}, of $(PCL_{29})_2$-*b*-$PDMA_{45}$, PCL_{61}-*b*-$(PDMA_{24})_2$, and PCL_{61}-*b*-$(PDMA_{24})_2$ micelles were then calculated to be 41, 120, and 247, respectively. The LLS results are summarized in Table 2.

Generally, the dependence of N_{agg} on the length of the insoluble block is stronger than that of the soluble block for linear diblock copolymers. An increase of N_{agg}, as the molecular weight and weight fraction of the insoluble block increase, has been predicted theoretically and verified experimentally in the micellization of other block copolymer systems.[1] In our case, all three types of copolymers have comparable composition and molecular weights (see Table 1). Thus the formation of micelles with different sizes and aggregation numbers must be due to the difference in topological arrangement of polymer chains, i.e., the chain architectural effects. Our results agrees fairly well with those obtained by Pispas et al.[20] They studied the micellar properties of PS-*b*-$(PI)_2$, $(PS)_2$-*b*-PI, and PS-*b*-PI copolymers in *n*-decane, a selective solvent for the PI block. The aggregation number and size of the PS-core micelles increased in the order PS-*b*-$(PI)_2$ < $(PS)_2$-*b*-PI < PS-*b*-PI. Based on the simple scaling theory developed by them,[20] the branching of the insoluble PCL block or soluble PDMA block increased the elastic energy of the stretching of the insoluble PCL block inside the micellar core, compared to that of the linear diblock copolymer. Thus the aggregation number needs to decrease to compensate the fixed gain in the aggregation energy.

Table 2. Characterization of Micelles Prepared from $(PCL_{29})_2$-*b*-$PDMA_{45}$ and PCL_{61}-*b*-$(PDMA_{24})_2$ Miktoarm Star Copolymers and PCL_{56}-*b*-$PDMA_{49}$ Linear Block Copolymer in Aqueous Solution

Samples	M_w[a]	$\langle R_h \rangle$[b] (nm)	μ_2/I^2[b]	$M_{w,app}$[c]	N_{agg}[d]	ρ[e] (g/cm^3)
$(PCL_{29})_2$-*b*-$PDMA_{45}$	15,800	17	0.09	1.9×10^6	120	0.15
PCL_{56}-*b*-$PDMA_{49}$	17,000	21	0.07	4.2×10^6	247	0.18
PCL_{61}-*b*-$(PDMA_{24})_2$	16,900	11	0.13	7.0×10^5	41	0.21

[a] The weight–average molecular weight of block copolymers, calculated from M_n determined by ^{1}H NMR and M_w/M_n determined by GPC.
[b] Determined by dynamic LLS at a concentration of 0.1 g/L, the estimated error associated with each value was $\pm$2 nm.
[c] The apparent molecular weight of PCL-core micelles, determined by static LLS at a concentration of 0.1 g/L.
[d] Calculated as: $N_{agg} = M_{w,app}/M_w$.
[e] The micelle density, calculated as: $\rho = M_{w,app}/(4\pi/3\langle R_h \rangle^3)$.

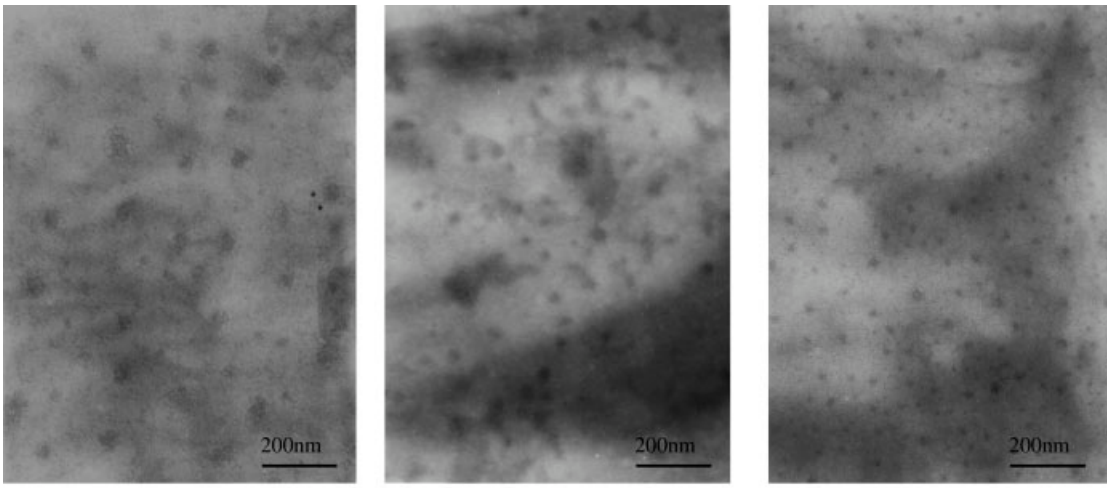

Figure 8. TEM images of the micelles prepared from PCL_{56}-*b*-$PDMA_{49}$ (a), $(PCL_{29})_2$-*b*-$PDMA_{45}$ (b), and PCL_{61}-*b*-$(PDMA_{24})_2$ (c) at a final concentration of 0.1 g/L.

Transmission electron microscopy (TEM) observations were performed to examine the actual morphologies of the micelles formed from these three types of copolymers. All of the images clearly revealed the presence of spherical nanoparticles of around 10–25 nm in diameter. Their sizes were in the order PCL_{61}-*b*-$(PDMA_{24})_2$ [Fig. 8(c)] < $(PCL_{29})_2$-*b*-$PDMA_{45}$ [Fig. 8(b)] < PCL_{56}-*b*-$PDMA_{49}$ [Fig. 8(a)], which is comparable to the sequence of micelle dimensions as determined by dynamic LLS. TEM determines the micelle dimensions in the dry state, while dynamic LLS report the intensity–average dimensions of micelles in solution which contains the contribution of the swollen PDMA corona, and so it is understandable that the micelle sizes determined by TEM were systematically smaller than that determined by LLS.

To get more information on the structural parameters of the micelles, the PCL-core radius, R_{core}, was calculated based on eq 2,[20] where wt_{PCL} is the weight fraction of PCL in the copolymer, N_A is the Avogadro number, d_{PCL} is the density of PCL, and Φ_{PCL} is the volume fraction of PCL in the micelle core. Φ_{PCL} can be assumed to be 1, i.e., the core is solvent-free, which is reasonable considering that PCL is highly hydrophobic.[78] d_{PCL} was taken as 1.13 g/cm^3 as found in the literature.[79] The thickness of the micelle corona, R_{corona}, can then be calculated from the differences in $\langle R_h \rangle$ and R_{core} based on eq 3. The area per junction point or per copolymer chain at the core–corona interface, A_c, can be calculated based on eq 4.

$$R_{core} = \left(\frac{3 M_{w,app} wt_{PCL}}{4\pi N_A d_{PCL} \Phi_{PCL}} \right)^{1/3} \quad (2)$$

$$R_{corona} = \langle R_h \rangle - R_{core} \quad (3)$$

$$A_c = \frac{4\pi R_{core}^2}{N_{agg}} \quad (4)$$

Table 3. Geometrical Parameters of Micelles Formed from $(PCL_{29})_2$-*b*-$PDMA_{45}$ and PCL_{61}-*b*-$(PDMA_{24})_2$ Miktoarm Star Copolymers and the PCL_{56}-*b*-$PDMA_{49}$ Linear Block Copolymer in Dilute Aqueous Solution

Samples	R_{core} (nm)[a]	R_{corona} (nm)[b]	A_c (nm^2)[c]	A_c/n (nm^2)[d]
$(PCL_{29})_2$-*b*-$PDMA_{45}$	6.8	10.2	4.8	4.8
PCL_{56}-*b*-$PDMA_{49}$	8.9	12.1	4.0	4.0
PCL_{61}-*b*-$(PDMA_{24})_2$	4.8	6.2	7.1	3.6

[a] Calculated based on eq 2.
[b] Calculated based on eq 3.
[c] Calculated based on eq 4.
[d] n is the number of soluble PDMA bocks per junction point at the core/corona interface.

The calculated geometrical characteristics for the three types of micelles, R_{core}, R_{corona}, and A_c, are summarized in Table 3. We can see that R_{core} increased in the order PCL_{61}-*b*-$(PDMA_{24})_2$ < $(PCL_{29})_2$-*b*-$PDMA_{45}$ < PCL_{56}-*b*-$PDMA_{49}$, following the same trend as that of N_{agg}. The corona thickness of $(PCL_{29})_2$-*b*-$PDMA_{45}$ and PCL_{56}-*b*-$PDMA_{49}$ are considerably larger than that of PCL_{61}-*b*-$(PDMA_{24})_2$, which is reasonable considering that the DP of the PDMA arms in the latter case is nearly halved compared to the former two copolymers. Compared to the size of free PDMA chains with similar DPs in water,[80] we can conclude that PDMA chains at the micelle corona take a relatively extended conformation due to steric exclusions imposed by neighboring PDMA chains at the corona.

Because of the crowding of polymer branches at the junction point, a larger surface area per copolymer chain at the core–corona interface was expected to accommodate the two PCL arms of $(PCL_{29})_2$-*b*-$PDMA_{45}$ or two PDMA arms of PCL_{61}-*b*-$(PDMA_{24})_2$ in an equilibrium conformation. Thus it was reasonable to observe that PCL_{56}-*b*-$PDMA_{49}$ micelles had the smallest surface area occupied per copolymer chain (A_c). If A_c was divided by the number of soluble PDMA arms per junction point (n), the surface area occupied per soluble PDMA block, A_c/n, can be calculated. PCL_{61}-*b*-$(PDMA_{24})_2$ micelles had the smallest A_c/n value, while $(PCL_{29})_2$-*b*-$PDMA_{45}$ micelles have the largest one (Table 3). From Table 2, we can also observe that PCL_{61}-*b*-$(PDMA_{24})_2$ and $(PCL_{29})_2$-*b*-$PDMA_{45}$ micelles had the largest and smallest overall micelle densities, respectively. As suggested by Pispas et al.,[20] the presence of two soluble arms at the junction point favors the bending of the core–corona interface toward the core and thus the micelle formation. Furthermore, we can also expect that the presence of two insoluble PCL blocks in the case of $(PCL_{29})_2$-*b*-$PDMA_{45}$ will make the formation of core-shell nanostructures less favorable and the core packing less compact, leading to lower micelle densities (Table 2).

CONCLUSIONS

In summary, well-defined amphiphilic PCL-*b*-$(PDMA)_2$ and $(PCL)_2$-*b*-PDMA Y-shaped miktoarm star copolymers and PCL-*b*-PDMA linear diblock copolymer were synthesized by a combination of ring-opening polymerization (ROP) and atom transfer radical polymerization (ATRP), where PCL is poly (ε-caprolactone) and PDMA is poly(2-(dimethylamino)ethyl methacrylate). All of the three types of copolymers have comparable PCL contents and overall molecular weights. These three amphiphilic copolymers self-assemble into PCL-core micelles in aqueous media. The chain architectural effects on the micellization properties, including the aggregation number, size, polydispersity, and micelle densities, of the amphiphilic copolymers in dilute aqueous solution were thoroughly explored by a combination of dynamic and static laser light scattering (LLS). The intensity–average hydrodynamic radius, $\langle R_h \rangle$, the aggregation number per micelle, N_{agg}, and the core radius, R_{core}, of the PCL-core micelles all increased in the order PCL_{61}-*b*-$(PDMA_{24})_2$ < $(PCL_{29})_2$-*b*-$PDMA_{45}$ < PCL_{56}-*b*-$PDMA_{49}$. The surface area occupied per soluble PDMA block at the core/corona interface increased in the order PCL_{61}-*b*-$(PDMA_{24})_2$ < PCL_{56}-*b*-$PDMA_{49}$ < $(PCL_{29})_2$-*b*-$PDMA_{45}$. PCL_{61}-*b*-$(PDMA_{24})_2$ micelles had the largest overall micelle density. An explanation for the chain architectural effects on the micellar properties of linear and nonlinear block copolymers was tentatively proposed.

This work was financially supported by an Outstanding Youth Fund (50425310) and research grants (20534020, 20674079) from the National Natural Scientific Foundation of China (NNSFC), the "Bai Ren" Project of the Chinese Academy of Sciences, and the Program for Changjiang Scholars and Innovative Research Team in University (PCSIRT).

REFERENCES AND NOTES

1. Tuzar, Z.; Kratochvil, P. Micelles of Block and Graft Copolymers in Solutions in Surface and Colloid Science; Plenum: New York, 1993.
2. Colfen, H. Macromol Rapid Commun 2001, 22, 219.
3. Gohy, J. F. Adv Polym Sci 2005, 190, 65.
4. Riess, G. Prog Polym Sci 2003, 28, 1107.
5. Lutz, J. F. Polym Int 2006, 55, 979.
6. Hawker, C. J.; Wooley, K. L. Science 2005, 309, 1200.
7. Thurmond, K. B.; Kowalewski, T.; Wooley, K. L. J Am Chem Soc 1997, 119, 6656.
8. Forder, C.; Patrickios, C. S.; Armes, S. P.; Billingham, N. C. Macromolecules 1996, 29, 8160.
9. Cameron, N. S.; Corbierre, M. K.; Eisenberg, A. Can J Chem 1999, 77, 1311.
10. Tezuka, Y.; Oike, H. J Am Chem Soc 2001, 123, 11570.
11. Hadjichristidis, N.; Iatrou, H.; Pitsikalis, M.; Pispas, S.; Avgeropoulos, A. Prog Polym Sci 2005, 30, 725.

12. Hadjichristidis, N.; Pispas, S. Adv Polym Sci 2006, 200, 37.
13. Xu, R. L.; Winnik, M. A.; Riess, G.; Chu, B.; Croucher, M. D. Macromolecules 1992, 25, 644.
14. Cai, Y. L.; Armes, S. P. Macromolecules 2005, 38, 271.
15. Cai, Y. L.; Tang, Y. Q.; Armes, S. P. Macromolecules 2004, 37, 9728.
16. Durmaz, H.; Karatas, F.; Tunca, U.; Hizal, G. J Polym Sci Part A: Polym Chem 2006, 44, 3947.
17. Iatrou, H.; Willner, L.; Hadjichristidis, N.; Halperin, A.; Richter, D. Macromolecules 1996, 29, 581.
18. Lambeth, R. H.; Ramakrishnan, S.; Mueller, R.; Poziemski, J. P.; Miguel, G. S.; Markoski, L. J.; Zukoski, C. F.; Moore, J. S. Langmuir 2006, 22, 6352.
19. Mountrichas, G.; Mpiri, M.; Pispas, S. Macromolecules 2005, 38, 940.
20. Pispas, S.; Hadjichristidis, N.; Potemkin, I.; Khokhlov, A. Macromolecules 2000, 33, 1741.
21. Ryu, S. W.; Asada, H.; Watanabe, T.; Hirao, A. Macromolecules 2004, 37, 6291.
22. Kasko, A. M.; Pugh, C. Macromolecules 2006, 39, 6800.
23. Gido, S. P.; Lee, C.; Pochan, D. J.; Pispas, S.; Mays, J. W.; Hadjichristidis, N. Macromolecules 1996, 29, 7022.
24. Chen, J. F.; Wang, X. Z.; Liao, X. J.; Zhang, H. L.; Wang, X. Y.; Zhou, Q. F. Macromol Rapid Commun 2006, 27, 51.
25. Lee, J. S.; Quirk, R. P.; Foster, M. D. Macromolecules 2005, 38, 5381.
26. Jabbarzadeh, A.; Atkinson, J. D.; Tanner, R. I. Macromolecules 2003, 36, 5020.
27. Lee, J. H.; Goldberg, J. M.; Fetters, L. J.; Archer, L. A. Macromolecules 2006, 39, 6677.
28. Wang, X.; Xia, J.; He, J.; Yu, F.; Li, A.; Xu, J.; Lu, H.; Yang, Y. Macromolecules 2006, 39, 6898.
29. Hamley, I. W. The Physics of Block Copolymers; Oxford University Press: Oxford, 1998.
30. Hadjichristidis, N.; Pitsikalis, M.; Iatrou, H. Adv Polym Sci 2005, 189, 1.
31. Hadjichristidis, N.; Pitsikalis, M.; Pispas, S.; Iatrou, H. Chem Rev 2001, 101, 3747.
32. Huang, J. L.; Huang, X. Y.; Hu, W. B.; Lou, W. K. Sci China Ser B-Chem 1997, 40, 663.
33. Wei, J.; Huang, J. L. Macromolecules 2005, 38, 1107.
34. Angot, B.; Taton, D.; Gnanou, Y. Macromolecules 2000, 33, 5418.
35. Erdogan, T.; Gungor, E.; Durmaz, H.; Hizal, G.; Tunca, U. J Polym Sci Part A: Polym Chem 2006, 44, 1396.
36. Fragouli, P. G.; Iatrou, H.; Hadjichristidis, N.; Sakurai, T.; Hirao, A. J Polym Sci Part A: Polym Chem 2006, 44, 614.
37. Ge, Z. S.; Luo, S. Z.; Liu, S. Y. J Polym Sci Part A: Polym Chem 2006, 44, 1357.
38. Glaied, O.; Delaite, C.; Dumas, P. J Polym Sci Part A: Polym Chem 2006, 44, 1796.
39. Heise, A.; Trollsas, M.; Magbitang, T.; Hedrick, J. L.; Frank, C. W.; Miller, R. D. Macromolecules 2001, 34, 2798.
40. Teng, J.; Zubarev, E. R. J Am Chem Soc 2003, 125, 11840.
41. Xu, J.; Zubarev, E. R. Angew Chem Int Ed Engl 2004, 43, 5491.
42. Zubarev, E. R.; Xu, J.; Gibson, J. D.; Sayyad, A. Org Lett 2006, 8, 1367.
43. Hedrick, J. L.; Trollsas, M.; Hawker, C. J.; Atthoff, B.; Claesson, H.; Heise, A.; Miller, R. D.; Mecerreyes, D.; Jerome, R.; Dubois, P. Macromolecules 1998, 31, 8691.
44. Fragouli, P.; Iatrou, H.; Hadjichristidis, N.; Sakurai, T.; Matsunaga, Y.; Hirao, A. J Polym Sci Part A: Polym Chem 2006, 44, 6587.
45. Han, D. H.; Pan, C. Y. Eur Polym Mater 2006, 42, 507.
46. Li, Q. B.; Li, F. X.; Jia, L.; Li, Y.; Liu, Y. C.; Yu, J. Y.; Fang, Q.; Cao, A. M. Biomacromolecules 2006, 7, 2377.
47. Hawker, C. J.; Bosman, A. W.; Harth, E. Chem Rev 2001, 101, 3661.
48. Yu, X. F.; Shi, T. F.; Zhang, G.; An, L. J. Polymer 2006, 47, 1538.
49. Miura, Y.; Narumi, A.; Matsuya, S.; Satoh, T.; Duan, Q.; Kaga, H.; Kakuchi, T. J Polym Sci Part A: Polym Chem 2005, 43, 4271.
50. Miura, Y.; Sakai, Y.; Yamaoka, K. Macromol Chem Phys 2005, 206, 504.
51. Miura, Y.; Yamaoka, K.; Mannan, M. A. Polymer 2006, 47, 510.
52. Guo, Y. M.; Pan, C. Y.; Wang, J. J Polym Sci Part A: Polym Chem 2001, 39, 2134.
53. Luan, B.; Zhang, B. Q.; Pan, C. Y. J Polym Sci Part A: Polym Chem 2006, 44, 549.
54. Tunca, U.; Ozyurek, Z.; Erdogan, T.; Hizal, G. J Polym Sci Part A: Polym Chem 2004, 42, 4228.
55. Durmaz, H.; Karatas, F.; Tunca, U.; Hizal, G. J Polym Sci Part A: Polym Chem 2006, 44, 499.
56. Erdogan, T.; Ozyurek, Z.; Hizal, G.; Tunca, U. J Polym Sci Part A: Polym Chem 2004, 42, 2313.
57. Genson, K. L.; Holzmueller, J.; Jiang, C. Y.; Xu, J.; Gibson, J. D.; Zubarev, E. R.; Tsukruk, V. V. Langmuir 2006, 22, 7011.
58. Voulgaris, D.; Tsitsilianis, C.; Esselink, F. J.; Hadziioannou, G. Polymer 1998, 39, 6429.
59. Voulgaris, D.; Tsitsilianis, C.; Grayer, V.; Esselink, F. J.; Hadziioannou, G. Polymer 1999, 40, 5879.
60. Penczek, S. Models of Biopolymers by Ring-Opening Polymerization; CRC Press: Boca Raton, FL, 1990.
61. Liu, S. Y.; Weaver, J. V. M.; Tang, Y. Q.; Billingham, N. C.; Armes, S. P.; Tribe, K. Macromolecules 2002, 35, 6121.
62. Deshpande, M. C.; Davies, M. C.; Garnett, M. C.; Williams, P. M.; Armitage, D.; Bailey, L.; Vamva-

kaki, M.; Armes, S. P.; Stolnik, S. J Controlled Release 2004, 97, 143.
63. Lam, J. K. W.; Ma, Y.; Armes, S. P.; Lewis, A. L.; Baldwin, T.; Stolnik, S. J Controlled Release 2004, 100, 293.
64. Rungsardthong, U.; Deshpande, M.; Bailey, L.; Vamvakaki, M.; Armes, S. P.; Garnett, M. C.; Stolnik, S. J Controlled Release 2001, 73, 359.
65. Jakubowski, W.; Matyjaszewski, K. Macromol Symp 2006, 240, 213.
66. Mespouille, L.; Degee, P.; Dubois, P. Eur Polym Mater 2005, 41, 1187.
67. Xu, Y. J.; Pan, C. Y.; Tao, L. J Polym Sci Part A: Polym Chem 2000, 38, 436.
68. Ge, Z. S.; Cai, Y. L.; Yin, J.; Zhu, Z. Y.; Rao, J. Y.; Liu, S. Y. Langmuir, in press.
69. Han, D. H.; Pan, C. Y. J Polym Sci Part A: Polym Chem 2006, 44, 2794.
70. Xu, J.; Ge, Z. S.; Zhu, Z. Y.; Luo, S. Z.; Liu, H.; Liu, S. Y. Macromolecules 2006, 39, 8178.
71. Guo, Y. M.; Xu, J.; Pan, C. Y. J Polym Sci Part A: Polym Chem 2001, 39, 437.
72. Luo, S. Z.; Xu, J.; Zhu, Z. Y.; Wu, C.; Liu, S. Y. J Phys Chem B 2006, 110, 9132.
73. Xu, J.; Luo, S. Z.; Shi, W. F.; Liu, S. Y. Langmuir 2006, 22, 989.
74. Pardo, L.; Osman, R.; Weinstein, H.; Rabinowitz, J. R. J Am Chem Soc 1993, 115, 8263.
75. Storey, R. F.; Sherman, J. W. Macromolecules 2002, 35, 1504.
76. Lee, S. B.; Russell, A. J.; Matyjaszewski, K. Biomacromolecules 2003, 4, 1386.
77. Li, Y. G.; Shi, P. J.; Pan, C. Y. Macromolecules 2004, 37, 5190.
78. Ganesh, R. N. a K. J Chem Phys 1989, 90, 5843.
79. Van de Velde, K.; Kiekens, P. Polym Test 2002, 21, 433.
80. Teraoka, I. Polymer Solutions: An Introduction to Physical Properties; Wiley: New York, 2002.